Since January 2020 Elsevier has created a COVID-19 resource centre with free information in English and Mandarin on the novel coronavirus COVID-19. The COVID-19 resource centre is hosted on Elsevier Connect, the company's public news and information website.

Available online at www.sciencedirect.com
ScienceDirect
Atmospheric Environment 41 (2007) 7473–7484
ATMOSPHERIC ENVIRONMENT
www.elsevier.com/locate/atmosenv

Study of expiratory droplet dispersion and transport using a new Eulerian modeling approach

Alvin C.K. Lai[a,*], Y.C. Cheng[b]

[a]Department of Building and Construction, City University of Hong Kong, Tat Chee Avenue, Kowloon, Hong Kong
[b]Carrier Transicold Pte Ltd, 251, Jalan Ahmad Ibrahim, Singapore 629146, Singapore

Received 3 November 2006; received in revised form 31 March 2007; accepted 23 May 2007

Abstract

Understanding of droplet nuclei dispersion and transport characteristics can provide more engineering strategies to control transmission of airborne diseases. Droplet dispersion in a room under the conventional well-mixed and displacement ventilation is simulated. Two droplet nuclei sizes, 0.01 and 10 μm, are selected as they represent very fine and coarse droplets. The flow field is modeled using k–ε RNG model. A new Eulerian drift-flux methodology is employed to model droplet phase. Under the conventional ventilation scheme, both fine and coarse droplets are homogeneously dispersed within approximately 50 s. Droplet nuclei exhibit distinctive dispersion behavior, particularly for low airflow microenvironment. After 270 s of droplet emission, gravitational settling influences the dispersion for 10 μm droplets, and concentration gradient can still be observed for displacement ventilation.

Keywords: Dispersion; Drift-flux model; Lagrangian model; Mixing; Ventilation

1. Introduction

After the outbreak of severe acute respiratory syndrome (SARS) and avian influenza in East and Southeast Asia, there has been increasing research interest in studying the transport and control of airborne bacteria and viruses indoors (Beggs et al., 2006; Chao and Wan, 2006; Li et al., 2007; Nicas et al., 2005) and in confined environments such as aircraft cabin (Mangili and Gendreau, 2005). Nosocomial transmission is also receiving significant attention in the medical literature (Tellier, 2006). In a review, Eickhoff (1994) estimated that as high as 10% of all hospital-acquired infections occurred through airborne transmission.

Transmission of airborne disease is a function of the concentration of respirable infectious particles in air and the contact time. When a contagious individual coughs or sneezes, droplets containing infectious particles (bacteria, viruses) are released. The larger ones fall to the floor within a few meters. Smaller droplets remain airborne long enough that the moist coating of saliva and mucus evaporate, leaving a residual dry nucleus of the droplet, that may include one or more bacteria or viruses (referred to droplet nuclei). By applying a simple water vapor balance calculation and using major components of mucus, Nicas et al. (2005) estimated

*Corresponding author. Tel.: +852 3442 6299; fax: +852 2788 7612.
E-mail address: alvinlai@cityu.edu.hk (A.C.K. Lai).

1352-2310/$ - see front matter © 2007 Elsevier Ltd. All rights reserved.
doi:10.1016/j.atmosenv.2007.05.045

the equilibrium diameter and the evaporating time required to reach the equilibrium state. Due to the presence of the nonvolatile compounds in mucus, the droplet nuclei equilibrium size is roughly half of the original droplet size and the evaporating time is in the order of 0.5 s. Similar finding is also reported by another review article (Morawska, 2006). Depending on the original (and final) size, droplet nuclei can remain suspended in air for several hours, hence they can travel over long distances, distribute widely throughout indoors, and lead to airborne transmitted infections.

Aerosol droplet dispersion and transport in a ventilated enclosure depend on the ventilation scheme, particle size, density, concentration, source location, etc. Among all the parameters, the ventilation scheme is the most important parameter influencing the droplet transport and dispersion indoors. The global airflow pattern affects significantly on the overall distribution of pollutants. High-level supply and high-level return (hereafter referred to well-mixed) scheme is the most popular ventilation arrangement for commercial buildings. High velocity, cooled air discharges through supply grills and warm air exhausts through return grills. For displacement ventilation systems low momentum, cooled air is supplied to lower part of the room and is exhausted through high ceiling return grills. Previous studies using passive gaseous as contaminant sources concluded that with heat sources, displacement ventilation is more favorable to remove the pollutants without mixing to the whole indoor environments (Brohus and Nielsen, 1996; He et al., 2005).

Droplet nuclei are aerosols, and some of their physical characteristics are very distinct from those of the gaseous counterparts. Gravitational deposition and inertia are among the most important characteristics that distinguish aerosols from gaseous, and the importance of both features increases with size. Nevertheless, some previous studies used passive gaseous as surrogates to investigate the transport and dispersion of aerosols (Beggs and Sleigh, 2002; Qian et al., 2006; Zhao et al., 2005) or applied well-mixed assumption to estimate the risk of droplet exposure (Nazaroff et al., 1998; Rudnick and Milton, 2003). Plausible reason of using gas surrogate is that generation of gaseous is relatively straightforward, and the detection is fairly simple with very high accuracy. On the other hand, generation and real-time detection of aerosol droplets concentration are more complicated.

Due to the complexity of the indoor airflow, the temporal and spatial distributions of droplet transport must be solved by computational fluid dynamics (CFD). Either Eulerian or Lagrangian frameworks can be employed to resolve the particulate phase. The author has developed a new Eulerian methodology (drift-flux model), and the model has been validated experimentally for a scaled chamber. Detailed descriptions of the model can be found elsewhere (Chen et al., 2006; Lai and Chen, 2006; Wang and Lai, 2006).

The key objectives of the present work are (i) to apply the new Eulerian approach to study droplet dispersion and transport in a ventilated room, and (ii) to highlight the influence of droplet sizes and ventilation scheme on mixing characteristics.

2. Case model description

To investigate droplet nuclei dispersion and transport using the new drift-flux approach, an enclosure with two identical model occupants with heat energy dissipated is selected (Fig. 1). There is one occupant emitting droplets (source) and faces directly to another occupant (receptor). The only differences between the well-mixed and displacement ventilation configurations are the inlet boundary conditions, location and geometry. For the well-mixed ventilation, a high-level supply grill is used while for displacement ventilation, a floor supply is employed. Table 1 shows the details of the room geometry and the boundary conditions. The geometry of a human occupant was originally suggested by Brohus and Nielsen (1996). An opening, 0.01×0.02 m, measured at 1.54 m above floor, locating at the centerline of the head is added to simulate the mouth of the occupant. Two planes are defined in the geometry; a breathing plane and a mid-plane. The breathing plane is 1.54 m above and parallel to the x–y plane. The mid-plane is symmetrical about the middle line in the x–z plane. Table 2 shows the details of the geometry of the model occupant used for this study. The wall temperature is set to 298 K while the surface of the model is specified by body temperature 309.5 K. It has been reported that the initial emission velocity can be up to 100 m s^{-1} (Wells, 1955). Recent study recording the coughed airflow of healthy males shows the velocity ranges from 6 to 22 m s^{-1} (Zhu et al., 2006). In the present study, the source emits unit density spherical droplet nuclei lasting for 0.5 s with initial velocity 50 m s^{-1}.

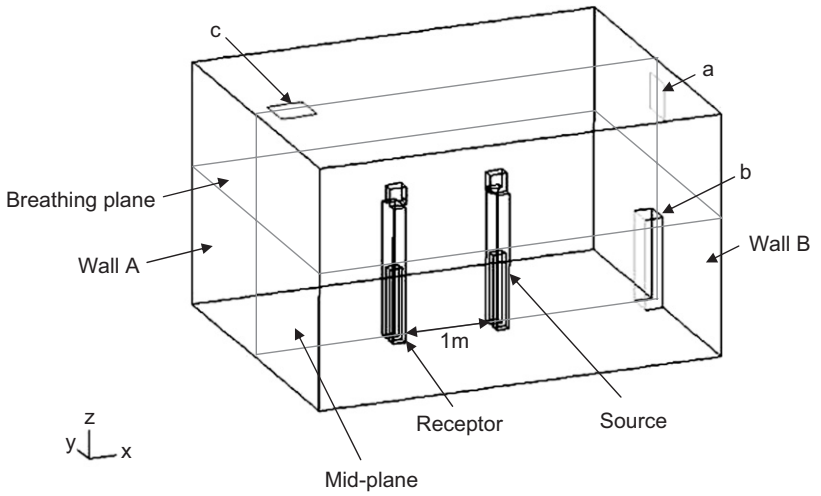

Fig. 1. Model room layout: (a) well-mixed inlet; (b) displacement inlet; (c) exhaust.

Table 1
Room configuration

	Location (m)			Size (m)			Temperature (K)	Volocity ($m\,s^{-1}$)
Name	X	Y	Z	ΔX	ΔY	ΔZ	–	–
Room	0	0	0	4.5	3.5	2.7	–	–
Well-mixed inlet (a)	4.5	1.75	2.1	–	0.4	0.4	287	2
Displacement inlet (b)	4.3	1.75	0	0.2	0.3	1	292	0.2
Exhaust (c)	0.2	1.75	2.7	0	0.4	0.4	–	–
Model (source)	1.58	1.75	0	–	–	–	–	–
Model (receptor)	1.48	1.75	0	–	–	–	–	–

Table 2
Geometry of the model occupant

Part	Dimensions (m)
Head	$0.18 \times 0.13 \times 0.2$
Torso	$0.14 \times 0.3 \times 0.7$
Leg	$0.14 \times 0.3 \times 0.8$
Mouth	0.01×0.02

Two recent review articles demonstrate the time scale of evaporation. Nicas et al. (2005) estimated that the shrinkage time from the original droplets to droplet nuclei is rapid and is in the order of 0.5 s. Morawska (2006) also draws similar conclusion showing a very rapid evaporation rate. She modeled three pure water droplet sizes, 1, 10 and 100 μm. For the two smaller droplet sizes, the time required to evaporate to the equilibrium size ranges from 0.001 to 0.4 s. This time scale is at least an order of magnitude shorter than the residence time of the droplet nuclei suspended in the room, hence the approach adopted here is to ignore the "evaporation period" and model the droplet nuclei directly.

Nicas et al. (2005) also summarized the droplet size data available from the literature, and the size ranges from submicron to over 1000 μm. It is understood that the expiratory droplets follows a certain size distribution, however, in this work, two representative droplet nuclei sizes, 0.01 and 10 μm, are chosen. The smaller size represents those fine droplets of which inertia and gravitational settling can be ignored, and their motions follow the air streamline. On the other hand, the coarse size represents the upper size limit that can be inhaled, deposited into lungs, and cause health problems. To simplify the model, the droplets are assumed trapped once they touch any surfaces and do not resuspend or break-up. These assumptions are valid for the present low air velocity environment. Coagulation effect has been examined by applying a simple estimation (Hinds, 1999). The particle

number and concentration selected are based on the review by Nicas et al. (2005). The result reveals that the coagulation effect can be neglected.

3. Numerical modeling

Renormalization Group (RNG) k–ε turbulent model is adopted here to simulate the airflow. The RNG k–ε model is more appropriate for indoor airflow simulation, and better agreement between simulated results and measured data has been achieved compared to the standard k–ε and other turbulence or laminar models (Chen, 1995; Posner et al., 2003).

A generic commercial CFD code FLUENT (Fluent, 2005) was used to simulate the airflow. The PISO algorithm was employed to couple the pressure and velocity fields. Grid independent tests were performed and the optimal grid densities for the well-mixed and displacement ventilation geometries are 404,000 and 375,000 cells, respectively. Since two dummy heat sources (occupants) are involved, there are buoyancy flows around the occupants. Here, air density is defined as a function of temperature by a piecewise-linear function. The simulation was performed on an SGI Onyx 3800 shared server.

3.1. Drift-flux approach

A simplified Eulerian drift-flux model has been developed to take full advantage of the extremely low volume fraction of indoor particles (Chen et al., 2006; Lai and Chen, 2006). The term "drift-flux" (or drift velocity) stands for particle flux (or velocity) caused by effects other than convection, i.e. gravitational settling and diffusion for the current work. The advantage of this approach is the feasibility of incorporating other external forces i.e. electrostatic (Wang and Lai, 2006) into the model. As the convective velocity of the particle phase is the same as the air phase, the complexity of the two-phase flow system is greatly reduced. The governing equation for particle transport in turbulent flow field is given as

$$\frac{\partial C_i}{\partial t} + \nabla \cdot [(\mathbf{u} + \mathbf{v}_{s,i})C_i] = \nabla \cdot [(D_i + \varepsilon_p)\nabla C_i] + S_{C_i}, \quad (1)$$

where $\mathbf{u}$ is the air phase velocity vector, C_i is the particle mass concentration, $\mathrm{kg\,m^{-3}}$ (or number concentration, $\mathrm{m^{-3}}$) of particle size group i (hereafter the subscription i denotes particle size group), $\mathbf{v}_{s,i}$ is the particle settling velocity, ε_p is the particle eddy diffusivity, and D_i is the Brownian diffusion coefficient and S_{C_i} is the mass concentration source term. The drift-flux methodology is incorporated into Fluent by a user-written sub-program.

3.2. Lagrangian approach

The performance of the new Eulerian model is compared with a Lagrangian approach, as discrete phase tracking has been employed to solve many types of two-phase engineering problems for more than a few decades. Zhao et al. (2005) conducted an order analysis and concluded that for indoor aerosol particles, only drag force, Brownian force and gravity, were important. The Lagrangian particle tracking is carried out by FLUENT built-in features. The equation of motion of a small aerosol particle can be written as

$$\frac{\mathrm{d}u_{p,i}}{\mathrm{d}t} = \frac{(u_i - u_{p,i})}{\tau} + n_i(t) + \frac{g_i(\rho_p - \rho)}{\rho_p}, \quad (2)$$

where $u_{p,i}$ and u_i are the velocity of the particle and fluid, respectively, τ is the particle relaxation time (Lai and Nazaroff, 2000), $n_i(t)$ is the Brownian force per unit mass, ρ_p and ρ are the particle and air density, respectively, and g_i is the gravitational acceleration. In the following section, some Eulerian and Lagrangian predictions will be presented side-by-side. For the Lagrangian approach, a sampling plane must be defined prior to counting the particles. Here, the droplets within 1.535–1.545 m (for breathing plane) and 1.745–1.755 m (for mid-plane) are selected. The purpose of including the Lagrangian approach is to compare the results qualitatively only. It must be emphasized here that direct quantitative comparison of these two approaches is impossible as the variables and governing equations solved are different.

4. Results and discussion

Fig. 2 shows the velocity field at the mid-plane for the two ventilation schemes at time "0" (momentarily before injection). For the well-mixed ventilation, the inlet jet flow causes air recirculation in the room, and the jet velocity is significantly higher than the neighboring region. In this figure, elapsed times which represent the arrival of the droplet puff to some specific locations are labeled. For instances,

under the well-mixed ventilation, the expiratory droplets takes approximately 0.5 s to reach the receptor's face, 2 s to reach the wall A, 5 s to the receptor's legs, 10 s to the wall B. All the above times mentioned refer to the elapsed times from the commencing of the droplet emitting process.

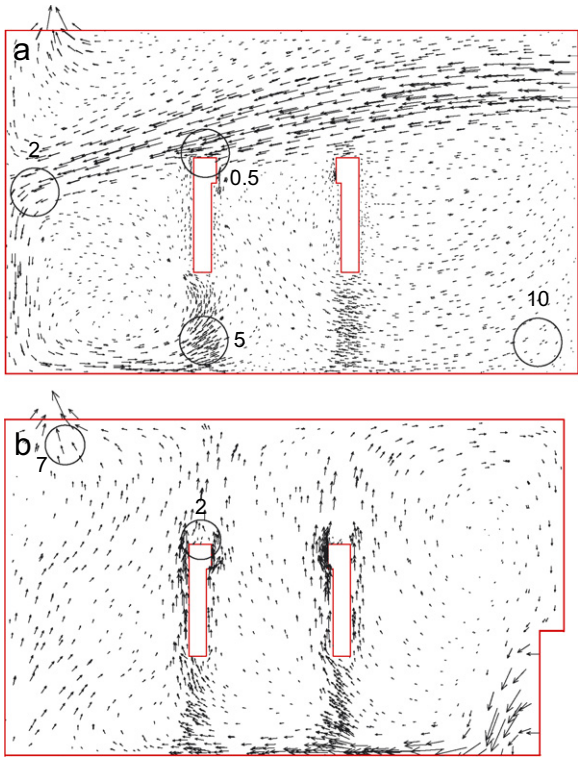

Fig. 2. Velocity magnitude at the mid-plane: (a) well-mixed ventilation; (b) displacement ventilation. The numeric shown in the figure indicates the time in second.

As expected, the displacement ventilation exhibits a very different airflow pattern. Cooled, low velocity air flows at near floor level absorbing heat from the two occupants, and a vertical thermal plume dominates the airflow field in the boundary layer around each occupant. Droplet cloud takes approximately 7 s to reach the exhaust. Except for the mid-plane, the airflow velocity is fairly weak in all other regions.

Although it is not the prime objective to study the statistical properties of the Lagrangian approach, a brief justification for the selection of the injection number seems necessary prior to discussing the results. Three injection numbers were tested; 3000, 10,000 and 90,000. Particles escaped through the outlet and deposited to the receptor's head region were recorded and counted. Inferring from Fig. 3, there is no statistical difference between the results of 10,000 and 90,000 injections. Hence, 10,000 injections were selected for all Lagrangian simulations.

Fig. 4 shows the combined results modeled by the drift-flux and Lagrangian approaches at the breathing plane and the mid-plane for 0.75 and 2 s elapsing from the commencing of the droplet emitting process. The high-speed droplet nuclei emitted from the mouth opening carry high momentum. They impact to the face of receptor directly resulting in significant particle loss. Inferring from the results, it can be observed that the two approaches predict

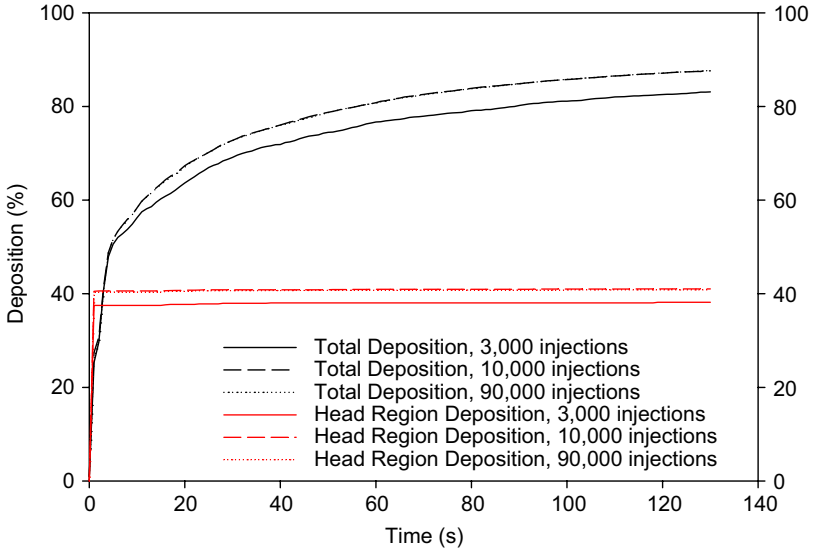

Fig. 3. Lagrangian simulation of droplets total deposition and onto the receptor's head under the well-mixed ventilation scheme.

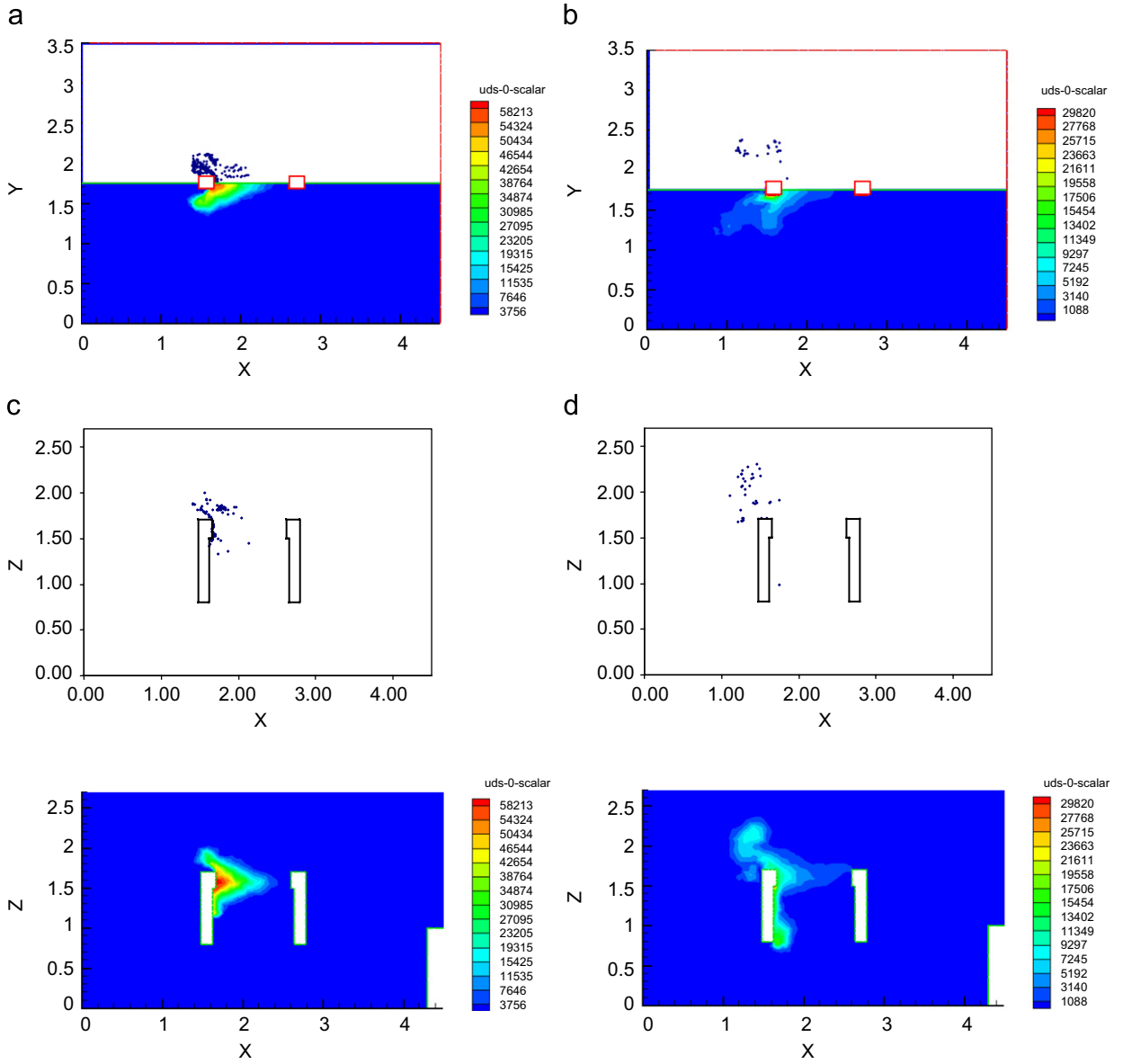

Fig. 4. Lagrangian and Eulerian combined plots for 0.01 droplets: under displacement ventilation (a) 0.75 s at breathing plane; (b) 2 s at breathing plane; (c) 0.75 s at mid-plane; (d) 2 s at mid-plane. The legend for the Eulerian plots represents the concentration magnitude.

fairly similar profiles, and the essential feature of the droplet dispersion is captured by the current Eulerian model.

Fig. 5 depicts the mid-plane results for 0.01 μm and 10 μm droplets under both ventilation schemes at 5 and 10 s. It is found out that for the same ventilation scheme, the difference between the two droplet sizes is not significant. The two modeling approaches give close matches, but this time the number of particles tracked are much less than those in Fig. 3.

As mentioned, the droplet dispersion depends on the bulk air movement and the physical properties of the droplet itself. The insignificant difference between two droplet sizes is attributed to the relatively short elapsed time presented here. Even for 10 μm droplets with unit density, the settling velocity is just $3 \times 10^{-3}\,\mathrm{m\,s^{-1}}$, hence it needs very long time to distinguish the dispersion characteristics (cf. Fig. 7). At those elapsed times reported, the droplet trajectories follow closely to the airflow pattern (cf. Fig. 2). For instances at 5 s for well-mixed

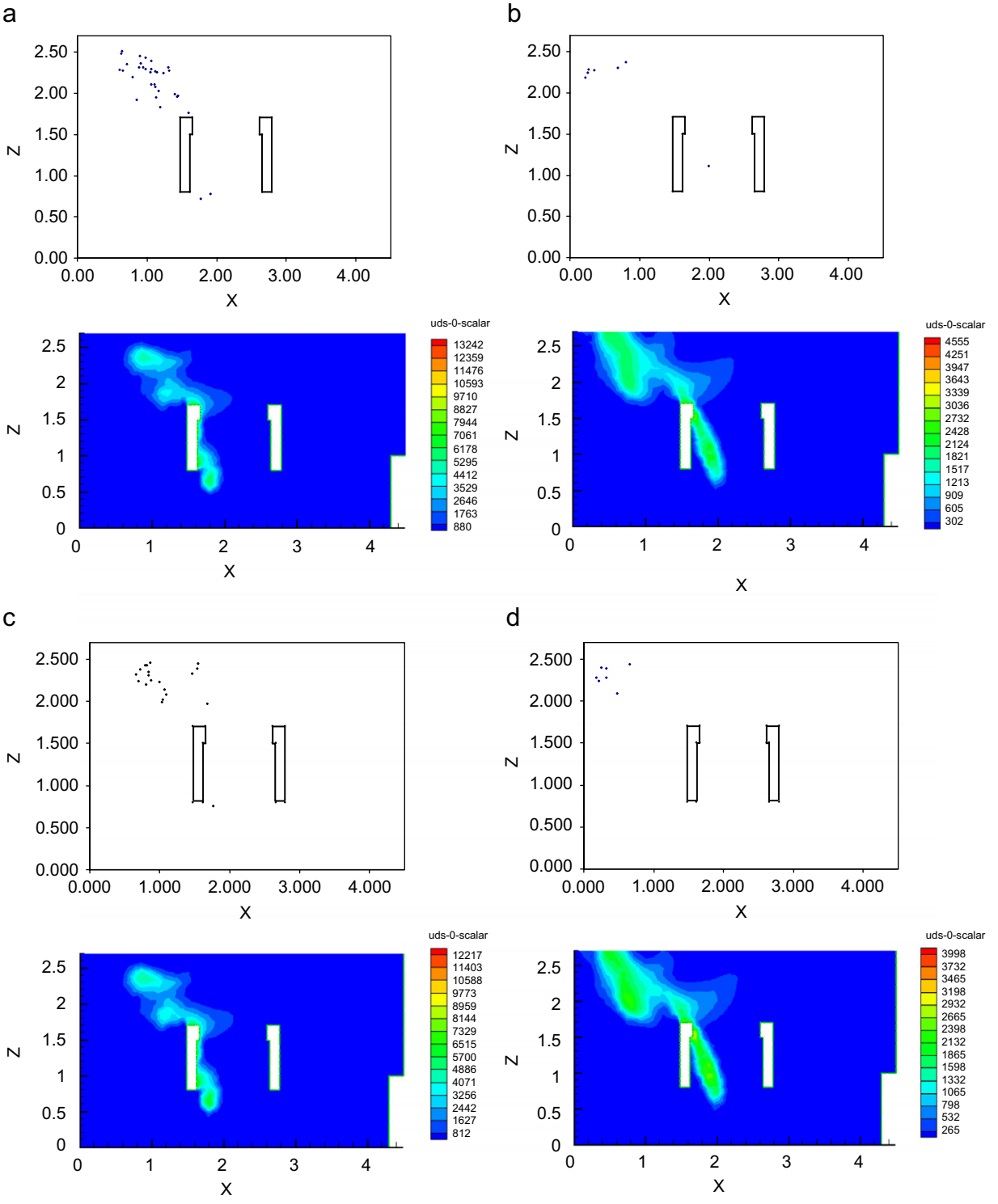

Fig. 5. Lagrangian and Eulerian plots at mid-plane for 0.01 and 10 μm droplets: (a) 0.01 μm, 5 s for displacement ventilation; (b) 0.01 μm, 10 s for displacement ventilation; (c) 10 μm, 5 s for displacement ventilation; (d) 10 μm, 10 s for displacement ventilation; (e) 0.01 μm, 5 s for well-mixed ventilation; (f) 0.01 μm, 10 s for well-mixed ventilation; (g) 10 μm, 5 s for well-mixed ventilation; (h) 10 μm, 10 s for well-mixed ventilation.

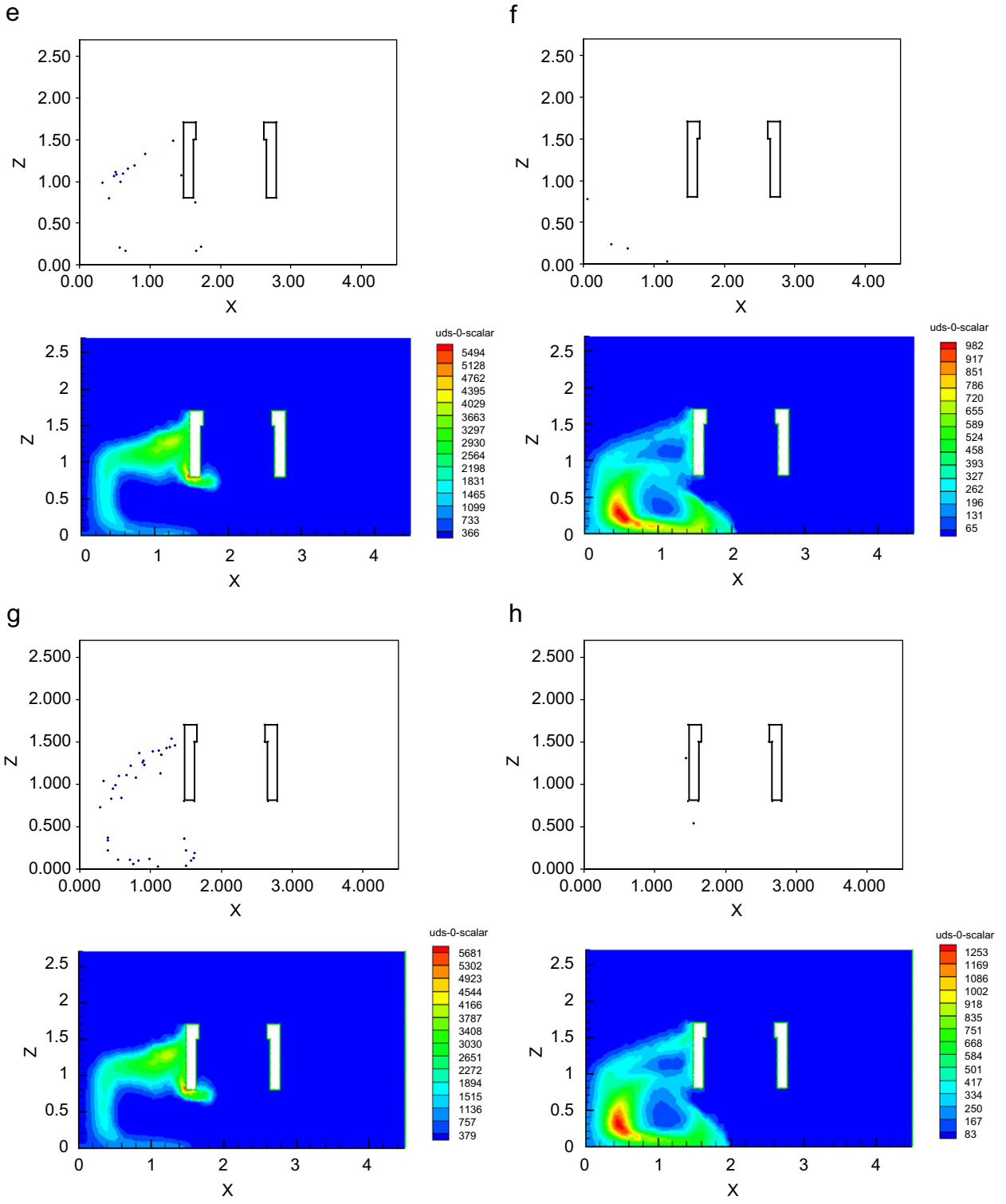

Fig. 5. (*Continued*)

ventilation, the puff just arrives at the receptor's legs, and it matches very closely to the bulk airflow pattern. Once the droplets are emitted, due to the much lower surrounding airflow speed they encountered, the droplets start to decelerate to attain the same velocity as the surrounding air, and then thereafter considered to be airborne. Particle relaxation time (τ) is used to characterize the time required for the particle to "relax" to become airborne

$$\tau = \frac{C_c d_p^2 \rho_p}{18\mu}, \tag{3}$$

where C_c is Cunningham slip correction factor, d_p is the droplet diameter, and μ is the kinematics viscosity of air. For the present system, the relaxation time ranges from 10^{-4} to 10^{-10} s. With these negligible relaxation times, the droplets decelerate almost instantaneously, and hence the droplets follow closely the airflow.

As expected the concentration profile is significantly different between the two ventilation schemes. For the well-mixed scheme, due to the much higher airflow velocity (in the x-direction) compared to the displacement scheme ($2\,m^{-1}$ s vs. $0.2\,m\,s^{-1}$), the droplets reach the vertical wall A in approximately 2 s. After the impact, many droplets are deposited to the wall, and the rest follows the large recirculation eddy. The predictions are very different for the displacement ventilation. In contrast to the well-mixed scheme where the airflow in x-direction dominates, the velocity in x-direction is very slow for the displacement ventilation. Due to this characteristic, the transport of droplets in that direction is fairly weak, and the droplets move slowly to the exhaust outlet.

Fig. 6 shows the dispersion at 50 s for the two ventilation schemes at the mid-plane; under the well-mixed scheme, 0.01 μm droplets are well-mixed, whereas large concentration gradient can still be observed under the displacement ventilation. In fact, the droplets do not disperse to most regions of the room until 270 s (refers to Fig. 7). Under such a single emission event studied here, droplets under displacement ventilation take approximately 14 times longer than that for the well-mixed ventilation to achieve moderate room dispersion.

Some salient features regarding the two approaches are worth discussion. First, under the Lagrangian methodology each particle has a unique ID, and hence the position for each particle can be tracked throughout the entire simulation domain and time. In risk exposure applications, this feature seems attractive only for some cases such as to investigate the individual "contribution" of multiple sources. For a single source, particle tracking feature is not important most of the time. Instead, for many exposure assessments, the spatial and temporal concentration levels are the vital pieces of information needed. Due to its discrete phase nature, the post-processing of the Lagrangian simulation for the results shown in Figs. 4, 5 and 7 is not trivial. In these figures, a 1-cm thick "slice" is chosen and particles enclosed in the slice are counted. If a thicker slice is chosen, it cannot represent the correct spatial concentration; on the other hand, if the slice is too thin, there may be no particle contained. The selection is, however, quite arbitrary. There is one transformation methodology, called particle-source-in-cell (PSIC), which can convert the discrete particle trajectories into concentration (Crowe et al., 1977). By using the residence time the particle stays in a pre-determined cell volume, the particle mass flow rate can be transformed to concentration. However, particle trajectories are still required prior to applying the transformation. This means that the accuracy of the transformation depends critically on the number of the injections. In contrast, since the droplet phase is treated as a continuum, the drift-flux approach can directly present the concentration magnitude over the entire spatial domain. This feature is very attractive for exposure assessment. Secondly, due to the nature of the governing equations resolved, direct comparison between Lagrangian and Eulerian results is impossible. Here a qualitative comparison is performed by counting the "discrete particles" in Fig. 5 and comparing to the scalar magnitude. Thirty three, 7, 17 and 10 are counted in the 1-cm slices of Figs. 5(a)–(d), respectively, and the trend is consistent with the scalar legend. In the future, more comprehensive comparison can be made by performing volume integration to get the spatial-average concentration.

Fig. 7 depicts the mid-plane results by the Lagrangian and drift-flux approaches at 210 and 270 s. Since the droplets are already homogeneously mixed at 50 s for the well-mixed system which is presented in Fig. 5, only the results for displacement ventilation are shown. Due to the relatively few suspended droplets, for those Lagrangian simulation results, the slice thickness is increased to 5 cm. Apparent difference between the 0.01 and 10 μm is observed at these two longer elapsed times.

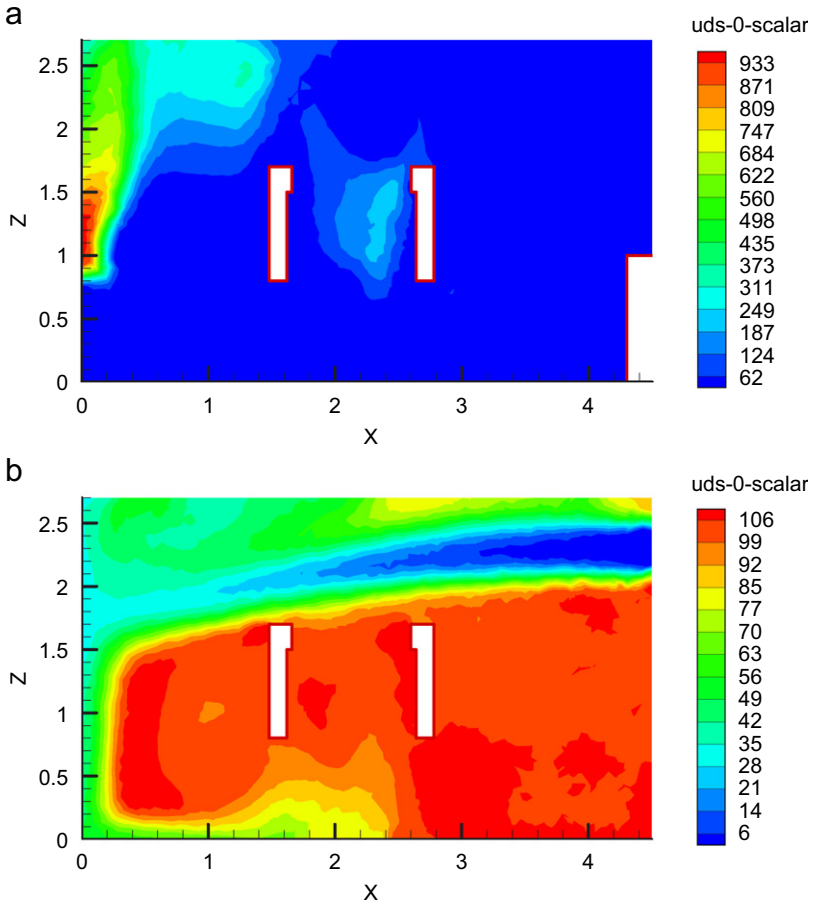

Fig. 6. Eulerian plots at mid-plane for 0.01 μm droplets at 50 s: (a) displacement ventilation: (b) well-mixed ventilation.

Sedimentation is observed for 10 μm particles as more droplets are found at the lower region, while for 0.01 μm particles no apparent settling is seen. In fact, a particle-free region is found for the 0.01 μm droplets. The same observation is found for the Lagrangian simulation for 10 μm: more discrete droplets can be found near ground level.

Literature results have shown similar conclusions. A recent study also shows that 3 μm particle concentration in a chamber exhibits inhomogeneity, and can be attributed by the turbulent diffusion and gravity (Richmond-Bryant et al., 2006). Chang et al. (2006) performed a detailed large eddy simulation on indoor particles under natural ventilation. He found out that, due to the larger inertia and gravitational settling, coarse particles (PM_{10}) can move easily from one circulation region to other ones while fine particles ($PM_{2.5}$) are easily influenced by the surrounding complex indoor air pattern.

Based on the literature and the current results, it reveals that droplet nuclei may exhibit distinctive dispersion behavior, particularly for low airflow microenvironment. Approximately about 40% of droplets are less than 10 μm in terms of number (Nicas et al., 2005). These droplets can still be inhaled and deposited deep to lungs. Hence, the present result has important implication; using passive gaseous as surrogates of droplet nuclei or applying the well-mixed assumption may cause incorrect exposure risk assessment results. In spite of the low relaxation time, deposition and gravitation effects may influence the accuracy if they are not properly taken into accounted.

5. Conclusions

An alternative Eulerian drift-flux model is adopted to simulate dispersion of droplet nuclei in a ventilated room. Two particle sizes (0.01 and

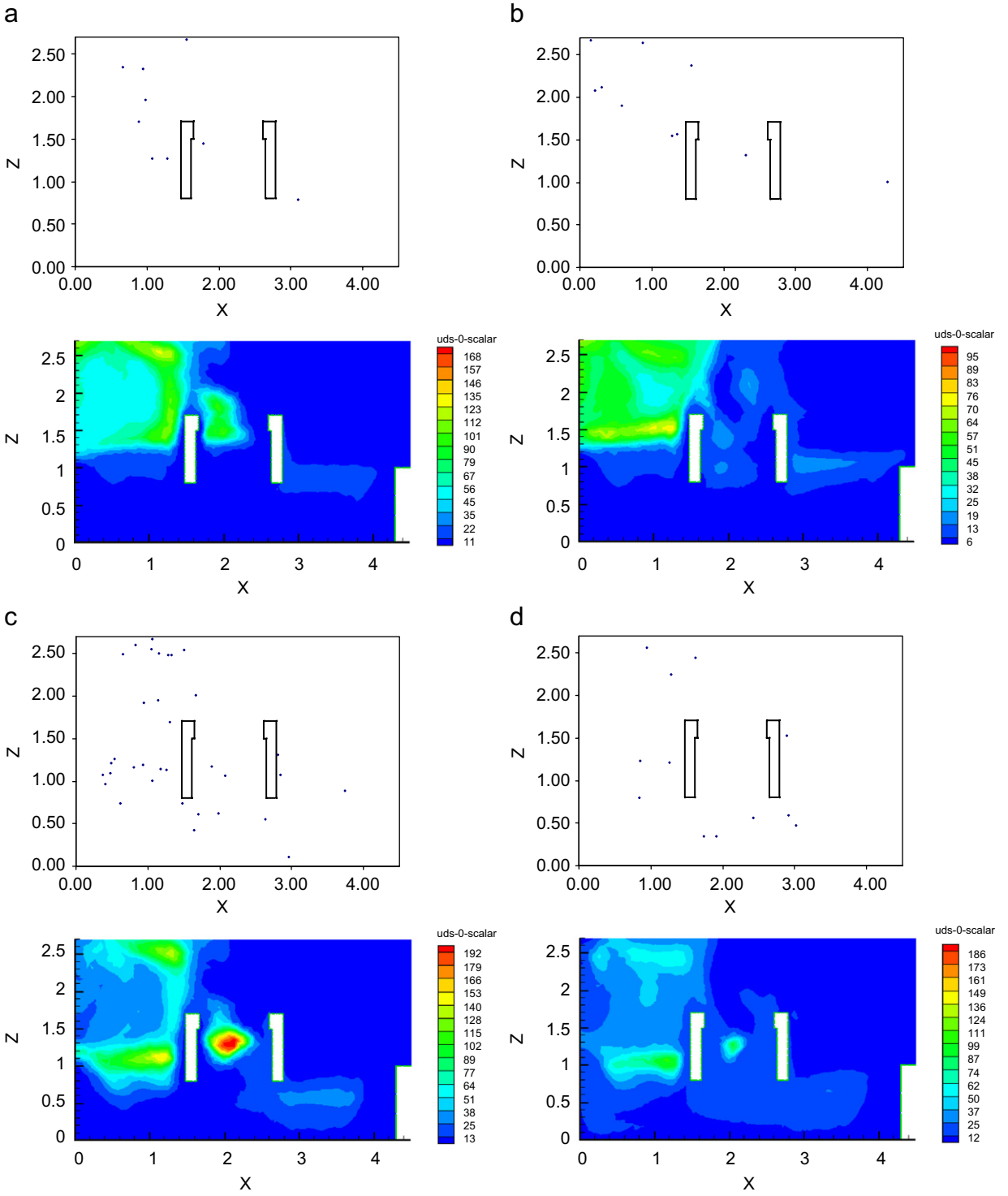

Fig. 7. Lagrangian and Eulerian plots at mid-plane under displacement ventilation: (a) 0.01 μm at 210 s; (b) 0.01 μm at 270 s; (c) 10 μm at 210 s; (d) 10 μm at 270 s.

10 μm) are chosen to mimic very fine and coarse droplet nuclei. Results show that both Lagrangian and drift-flux approaches give similar concentration profiles. However, there are a few inherent drawbacks for the Lagrangian approach including the difficulty in generating particle density plots at a certain plane, and more importantly the uncertainty in the number of droplets injected may lead to inaccurate conclusion, particularly if the number of droplet suspension is low. On the other hand, using the drift-flux approach with proper account on sedimentation gives straightforward concentration profile. In addition, the computational time and resources required for the drift-flux are much less than those required for the traditional Lagrangian particle tracking methodology (typically less than 50%). This advantage becomes more significant for complex geometries with substantial grid elements.

Inferring from the results presented, it can be observed that for the well-mixed ventilation scheme, the dispersion pattern is dominated by the high velocity airflow, and the different between droplet sizes is not obvious. The droplets are homogeneously mixed within 1 min. When the global airflow speed is lower, the distinctive characteristics of coarse size start to appear. Ten micrometer droplets begin to settle at the lower region of the room under displacement ventilation.

References

Beggs, C.B., Sleigh, P.A., 2002. A quantitative method for evaluating the germicidal effect of upper room UV fields. Journal of Aerosol Science 33, 1681–1699.

Beggs, C.B., Noakes, C.J., Sleigh, P.A., Fletcher, L.A., Kerr, K.G., 2006. Methodology for determining the susceptibility of airborne microorganisms to irradiation by an upper-room UVGI system. Journal of Aerosol Science 37, 885–902.

Brohus, H., Nielsen, P.V., 1996. Personal exposure in displacement ventilated rooms. Indoor Air 6, 157–167.

Chang, T., Hsieh, Y., Kao, H., 2006. Numerical investigation of airflow pattern and particulate matter transport in naturally ventilated multi-room buildings. Indoor Air 16, 136–152.

Chao, C.Y.H., Wan, M.P., 2006. A study of the dispersion of expiratory aerosols in unidirectional downward and ceiling-return type airflows using a multiphase approach. Indoor Air 16, 296–312.

Chen, Q., 1995. Comparison of different k–ε models for indoor airflow computations. Numerical Heat Transfer, Part A, Fundamentals 28, 353–369.

Chen, F., Yu, S.C.M., Lai, A.C.K., 2006. Modeling particle distribution and deposition in indoor environments with a new drift-flux model. Atmospheric Environment 40, 357–367.

Crowe, C.T., Sharma, M.P., Stock, D.E., 1977. The particle-source in cell method for gas droplet flow. ASME Journal of Fluids Engineering 99, 325–332.

Eickhoff, T.C., 1994. Airborne nosocomial infection: a contemporary perspective. Infection Control and Hospital Epidemiology 15, 663–672.

FLUENT Inc., 2005. FLUENT 6.2 User's Guide. Lebanon, NH.

He, G., Yang, X., Srebric, J., 2005. Removal of contaminants released from room surfaces by displacement and mixing ventilation: modeling and validation. Indoor Air 15, 367–380.

Hinds, W.L., 1999. Aerosol technology, second ed. Wiley-Interscience, New York.

Lai, A.C.K., Chen, F., 2006. Comparison of a new Eulerian model with a modified Lagrangian approach for particle distribution indoors. Atmospheric Environment, in press, doi:10.1016/j.atmosenv.2006.05.08.

Lai, A.C.K., Nazaroff, W.W., 2000. Modeling indoor particle deposition from turbulent flow onto smooth surfaces. Journal of Aerosol Science 31, 463–476.

Li, Y., Leung, G.M., Tang, J.W., Yang, X., Chao, C.Y.H., Lin, J.Z., Lu, J.W., Nielsen, P.V., Niu, J., Qian, H., Sleigh, A.C., Su, H.-J.J., Sundell, J., Wong, T.W., Yuen, P.L., 2007. Role of ventilation in airborne transmission of infectious agents in the built environment—a multidisciplinary systematic review. Indoor Air 17, 2–18.

Mangili, A., Gendreau, M.A., 2005. Transmission of infectious diseases during commercial air travel. Lancet 365, 989–996.

Morawska, L., 2006. Droplet fate in indoor environments, or can we prevent the spread of infection? Indoor Air 16, 335–347.

Nazaroff, W.W., Nicas, M., Miller, S.L., 1998. Framework for evaluating measures to control nosocomial tuberculosis transmission. Indoor Air 8, 205–218.

Nicas, M., Nazaroff, W.W., Hubbard, A., 2005. Toward understanding the risk of secondary airborne infection: emission of respirable pathogens. Journal of Occupational and Environmental Hygiene 2, 143–154.

Posner, J.D., Buchanan, C.R., Dunn-Rankin, D., 2003. Measurement and prediction of indoor air flow in a model room. Energy and Buildings 35, 515–526.

Qian, H., Li, Y., Nielsen, P.V., Hyldgaard, C.E., Wong, T.W., Chwang, A.T.Y., 2006. Dispersion of exhaled droplet nuclei in a two-bed hospital ward with three different ventilation systems. Indoor Air 16, 111–128.

Richmond-Bryant, J., Eisner, A.D., Brixey, L.A., Wiener, R.W., 2006. Transport of airborne particles within a room. Indoor Air 16, 48–55.

Rudnick, S.N., Milton, D.K., 2003. Risk of indoor infection transmission estimated from carbon dioxide concentration. Indoor Air 13, 237–245.

Tellier, R., 2006. Review of aerosol transmission of Influenza A virus. Emerging Infectious Diseases 12, 1657–1662.

Wang, J.B., Lai, A.C.K., 2006. A new drift-flux model for particle transport and deposition in human airways. Journal of Biomechanical Engineering 128, 97–105.

Wells, W.F., 1955. Airborne Contagion and Air Hygiene. Harvard University Press, Cambridge, MA (Chapter 1).

Zhao, B., Zhang, Z., Li, X., 2005. Numerical study of the transport of droplets or particles generated by respiratory system indoors. Building and Environment 40, 1032–1039.

Zhu, S., Kato, S., Yang, J-H., 2006. Study on transport characteristics of saliva droplets produced by coughing in a calm indoor environment. Building and Environment 41, 1691–1702.